

# A DFT Study of Interaction of (CdSe)<sub>3</sub> Quantum Dots with Nucleobases

Pragati Malik<sup>1</sup> and Rita Kakkar<sup>2,\*</sup> 

Deoxyribonucleic acid (DNA) and ribonucleic acid (RNA) play important roles in the storage of genetic information and protein biosynthesis. Nucleobases, which are nitrogenous bases, are the functional units of these nucleic acids. It is very important to detect changes in the sequence of DNA/RNA, as any mutations in them may cause harm to the organism. Our aim is to verify the use of (CdSe)<sub>3</sub> Quantum Dots (QDs), owing to their distinctive optical and electronic properties, for sensing changes in DNA/RNA. Hence, in this work, we have focused on studying the interaction between (CdSe)<sub>3</sub> QDs and the five nucleobases (adenine, guanine, cytosine, thymine and uracil) at various probable sites by means of density functional calculations. Several structural, electronic and optical properties, and charge transfer on interaction between the two, have been discussed. The present band gap and charge transfer calculations indicate that binding of (CdSe)<sub>3</sub> to guanine is strongest and is weakest with uracil. The vibrational spectral analysis indicates that the intensities of the peaks due to (CdSe)<sub>3</sub> enhance on interacting with the nucleobase, and a blue shift is observed in all the interactions. The presence of both the frontier orbitals (HOMO and LUMO) on the QD indicates that (CdSe)<sub>3</sub> acts as a guardian of DNA and prevents it from damage. Hence, our studies direct that CdSe QDs can be successfully employed as sensors for these nucleobases.

## Introduction

Nucleobases are nitrogen-containing biological compounds found in DNA and RNA. The helical structure of DNA and RNA is due to the ability of the nucleobases present in them to exist in the form of base-pairs through hydrogen bonds and stacking upon one another. Important nucleobases are adenine (A), guanine (G), cytosine (C), thymine (T) and uracil (U), out of which A, G, C are found in both DNA and RNA, T is found in DNA only, while U is found only in RNA. In the normal helical structure of DNA, bases form pairs sandwiched between the two strands, A with T and C with G through two and three hydrogen bonds, respectively. Any abnormality in the nucleobases leads to changes in organisms, both physiological and genetic, and hence various diseases in organisms. Therefore, it is remarkably desirable to develop diagnostic measures for analyzing these bases for promoting developments in bioscience and clinical diagnostic fields [1]. It is significant to build up innovative and cost-effective methods with high efficiency and convenience for the determination of these

nucleobases. Many methods, such as spectroscopic methods coupled with chromatography or electrophoresis [2,3], and electrophoresis with electrochemical detection [4,5], have been developed for the recognition and quantification of purine bases in nucleic acids.

Nowadays, nano-bio complexes have found use in various fields, such as biomedical engineering, which employs the engineering perception in medicine and biology from the health concern point of view [6-8], and nanoscale electronics, which employs the use of nanotechnology in electronics [9-12]. However, it is very important to pick nanoparticles with high biocompatibility and interactive functionality for applying them for these applications. The binding selectivity of inorganic nanoclusters may be modulated by combining them with various biomolecules, such as polypeptides or DNA [13-32]. This idea of altering the surface of nanoclusters suggests that we can employ them for sensing various biomolecules as well. Colloidal QDs represent one of the most appealing, broadly explored and studied systems in the field of semiconductor nanocrystals, predominantly due to the quantum confinement effect, owing to which their electronic and optical properties become strongly size-dependent [33]. In this respect, it is interesting to study CdSe, which is one of the most studied II-VI dots due to its ease of synthesis. Also, its optical gap can cover the whole visible spectrum [34], depending on the dimension of the QD. Various reports on the determination of the concentration of adenine and guanine in DNA using CdSe have been presented by different

<sup>1</sup>Computational Chemistry Laboratory, Department of Chemistry, University of Delhi, Delhi 110 007, India

<sup>2</sup>Department of Chemistry, University of Delhi, Delhi 110 007, India

\*Corresponding author:

E-mail: rkakkar@chemistry.du.ac.in; Tel.: (+91) 11 27666313

DOI: 10.5185/amlett.2021.081653

research groups experimentally as well as computationally in terms of the geometry, electronic structure, and electronic spectra [35-39]. Not only CdSe, but varieties of other quantum dots have also been employed for DNA recognition. The interaction of CdTe QDs with adenine and guanine results in enhanced photoluminescence [40,41]. CdS QDs also exhibit an increase in fluorescence in the presence of adenine, while it is quenched in the presence of guanine [42]. Fluorescence quenching of the QDs is observed when CdSe or CdTe QDs interacts with cytosine, guanine, or thymine [43]. A very well studied epigenetic alteration in humans, DNA methylation, which is considered as a biomarker for cancer detection [44-47], can be detected using CdTe QDs [48]. Highly luminous CdTe/ZnSe core/shell QDs have also been explored to distinguish purines from pyrimidines [49]. Recently, Li and coworkers have investigated the effect of the interaction of amino acids and quantum dots by examining the effect of interaction on the fluorescence and the optical activity of QDs where a significant fluorescence enhancement for L/D-Cys-CdTe QDs upon interaction with various amino acids was observed [50]. In another study, mechanism of DNA sensing was developed based on optical properties of graphene oxide (GO) and molybdenum disulphide (*MoS*2) nanopores, where GO and *MoS*2 were employed as quantum dot nanopore and DNA molecule translocate through the nanopore [51]. Fluorescence resonance energy transfer (FRET) system based on functionalized CdTe-guanine and AuNPs-cytosine bioconjugates for the nucleobase - guanine detection was developed to determine the free guanine concentration [52]. Structural stability, electronic, optical and vibrational properties of DNA nucleobase adsorbed graphene quantum dot have been examined using density functional theory. Based on electronic structure calculations, the predicted order of sensitivity for DNA nucleobase was found to be as Thymine > Cytosine > Guanine > Adenine [53]. The *in-situ* formation of CdS quantum dots integrated into a metallogel formed through the coordination of Cd<sup>2+</sup> with two pyrimidine nucleobases has been studied and found that thymine and uracil formed spontaneous hydrogels with nanofibrous morphology through coordinative interaction with Cd<sup>2+</sup> ions at alkaline pH [54]. Saha and Sarkar have carried out the theoretical investigation of the interaction of different nucleobases with ZnO nanoparticles [55].

Since it would be complicated and computationally expensive to carry out full scale quantum mechanical calculations with nucleic acid strands or complex nucleic acid structures, we have initiated computations with the nucleobases, the building blocks of the genetic macromolecules (DNA/RNA), in order to locate the factors essential in nano-bio interactions, and the changes produced in the CdSe QDs when these two interact, so that we can demonstrate their use as novel sensors for these nucleobases. In this work, the interaction

patterns of binding between the (CdSe)<sub>3</sub> QD and the five nucleobases (adenine, guanine, cytosine, thymine and uracil) in the neutral form have been investigated for the gas phase using DFT methods by considering only bare, spherical, stoichiometric (CdSe)<sub>3</sub> quantum dots for studying the changes produced on interaction in the above mentioned QDs with nucleobases at various possible sites.

## Computational details

First-principles density functional (DF) calculations [56] were performed by means of the DMol<sup>3</sup> code [57-61], obtained from Accelrys Inc. in the Materials Studio 4.4 package. DMol<sup>3</sup> employs numerical functions on an atom centered grid as its atomic basis. These basis sets were constructed specifically for use in DFT calculations. Their high quality minimizes superposition (BSSE) effects [57]. The long range tail of the basis set exhibits the correct charge allocation and allows an enhanced depiction of molecular polarizabilities [62]. We have employed numerical basis sets of double zeta quality plus polarization function (DNP). The DNP basis set is the numerical equivalent of the Gaussian basis, 6-31G\*\* [63]. All the structures were optimized using DFT–semilocal pseudopotentials [61] to define the cores. Hirshfeld's method was used to carry out charge partitioning [64] and covalent bond orders were calculated using Mayer's procedure [65].

## Results and discussion

We chose the smallest (CdSe)<sub>n</sub> wurtzite cluster and made it interact with various purine and pyrimidine bases in order to examine the structural and electronic changes produced in both when they interact at different orientations.

First, the geometrical structures of the isolated nucleobases and the (CdSe)<sub>3</sub> QD were optimized without symmetry constraints. Subsequently, the optimized structures were used to find out the preferred site of the interaction of the nucleobases with the (CdSe)<sub>3</sub> QD. For this, we selected all possible sites of each nucleobase where interaction with the QD may occur and compared the energies of the resulting complexes.

### (CdSe)<sub>3</sub> QD and the nucleobases

**Fig. 1(a)** shows the optimized structure of the (CdSe)<sub>3</sub> QD and the nucleobases. In the structure of (CdSe)<sub>3</sub> QD, it can be seen that all cadmium and selenium atoms are di-coordinated. The computed average Cd-Se bond length in (CdSe)<sub>3</sub> is 2.533 Å, which is smaller than the sum of ionic radii of the two ions (Cd<sup>2+</sup> and Se<sup>2-</sup>), i.e., 2.93 Å, demonstrating covalent character of the bonds in the hexagonal ring.

The nucleobases (purines and pyrimidines) are in association with their respective complementary base through hydrogen bonds; these base-pairs play a very

important role in biological systems. **Fig. 1(b)** shows the structures of the five nucleobases, adenine, guanine, cytosine, thymine, uracil with their standard atom numbering.

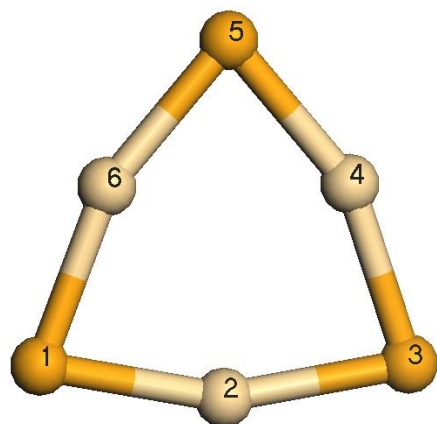


**Fig. 1(a).** Optimized structures of  $(\text{CdSe})_3$  QD.

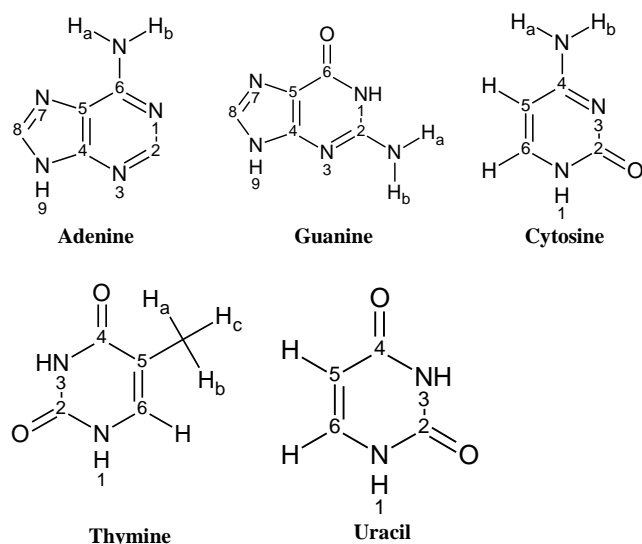


**Fig. 1(b).** Structures of the nucleobases.

The frontier orbitals, i.e., HOMO (Highest occupied molecular orbital) and LUMO (Lowest unoccupied molecular orbital), which are responsible for chemical reactivity, are shown in **Table 1** for all the structures examined here. The HOMOs of the bases comprise the  $\pi$  orbitals conjugated with the nitrogen lone pairs and the LUMOs are the  $\pi^*$  orbitals.

As shown in **Table 1**,  $(\text{CdSe})_3$  has a very low lying LUMO. It is, therefore, a good electron acceptor. On comparing with the HOMO energies of the nucleobases, it is apparent that none of the nucleobases can transfer electronic charge to the LUMO of the QD because their HOMO energies are much lower than the LUMO of the QD. The smallest energy gap (2.09 eV) is that between the HOMO of guanine and the LUMO of the QD, and thus the most favorable charge transfer should be from guanine to the QD.

**Table 1.** Calculated properties (eV) of the bare  $(\text{CdSe})_3$  QD and nucleobases.

	Binding energy (eV)	HOMO	LUMO
$(\text{CdSe})_3$	-10.40	-4.91	-2.42
Adenine	-77.28	-4.67	-0.76
Guanine	-82.75	-4.51	-0.55
Cytosine	-64.75	-4.81	-1.06
Thymine	-75.94	-5.24	-1.37
Uracil	-62.68	-5.41	-1.51

### Interaction of $(\text{CdSe})_3$ with nucleobases

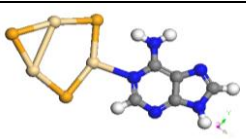
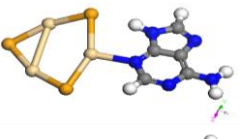
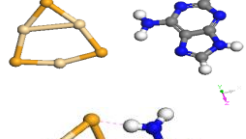
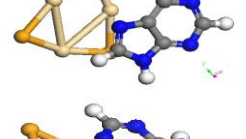
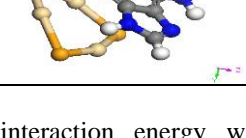
All the possible sites of interaction for each nucleobase with  $(\text{CdSe})_3$  were considered and the resultant bonding was studied in order to find out the preferred site for interaction between the two. The results are presented in the following sections.

#### $(\text{CdSe})_3$ -Adenine interaction

Five possible sites of interaction of adenine were considered, as shown in **Table 2(a)**, and the structural and electronic changes are reported in the sections that follow.



**Table 2(a).** Optimized structures of complexes between the (CdSe)<sub>3</sub> QD and adenine and their energies (eV).

Site	Final geometry	Interaction energy	HOMO	LUMO
N-site		0.41	-4.57	-1.89
NCN-site		0.53	-4.61	-1.95
NH <sub>2</sub> -site		-0.25	-5.04	-2.61
Five membered ring		-0.03	-4.97	-2.45
Six membered ring		0.04	-4.74	-2.34

The interaction energy was calculated from the relation

$$E_{\text{interaction}} = [E(\text{qd}) + E(\text{nucleobase})] - [E(\text{qd-nucleobase})],$$

where  $E$  denotes the binding energy of the respective system. Positive values for the interaction energy imply exothermic interactions [66]. From **Table 2(a)**, it is clear that NCN and N are the preferred sites of interaction. In case of the former, the optimized structure shows bond formation between Cd2 and N3 of adenine (bond order = 0.287), along with one Cd-Cd bond formation. The average Cd-Se bond length increases to 2.541 Å. The other favorable interaction is when adenine is placed such that the ring nitrogen (N1) adjacent to the amino group interacts with the cadmium atom of the QD (N site, **Table 2(a)**), and a bond is formed between Cd4 and N1 with bond order 0.277. One Cd-Cd bond is also formed with a bond length of 3.179 Å. In both cases, the covalency of cadmium is increased to three through metal-metal bond formation.

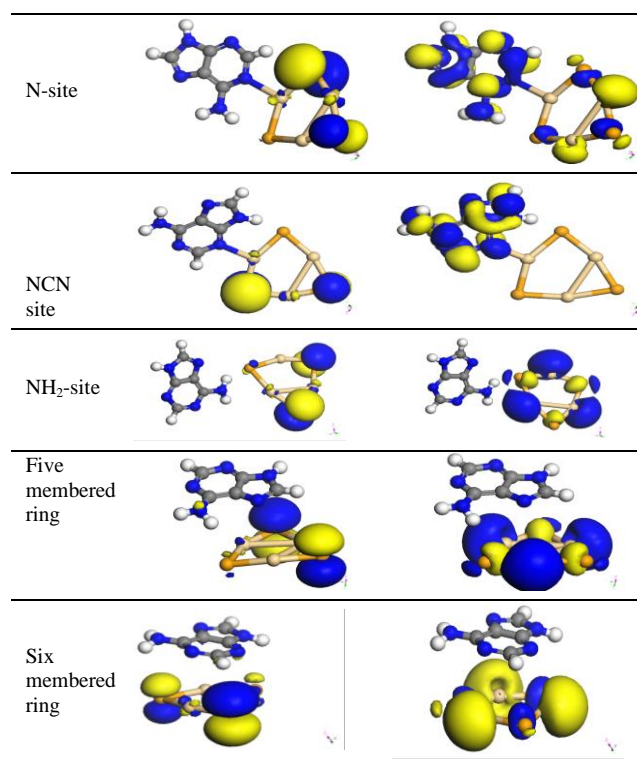
The calculated HOMO and LUMO energies of the structures after interaction are also shown in **Table 2(a)**. Comparing with **Table 1** for the uncomplexed QD and adenine, we observe that the HOMO energies are closer to, but slightly higher than, that of adenine (which has the higher HOMO), while the LUMO energies are closer to, but slightly higher than, that of (CdSe)<sub>3</sub> (which has the lower LUMO). This implies charge transfer to the LUMO of (CdSe)<sub>3</sub> from the HOMO of adenine, which raises the LUMO energy of the QD, increasing the HOMO-LUMO gap.

According to the energy viewpoint, the HOMO-LUMO gap of the resulting structure can be used as a director of kinetic stability. A smaller HOMO-LUMO gap implies lower kinetic stability and higher chemical reactivity due to energetically favorable addition of electrons to the low lying LUMO or extracting electrons from a high lying HOMO. The structures with large HOMO-LUMO gaps are generally stable and unreactive, while those with small gaps are generally reactive. Thus, according to the above criterion, interaction at the NCN- and N-sites, compared with five membered and six membered rings, is kinetically favored because of the increase in the HOMO-LUMO gaps (2.66 and 2.68 eV, respectively) compared to the bare QD (2.49 eV), as well as being thermodynamically favorable.

The Hirshfeld charge analysis for interaction of adenine with (CdSe)<sub>3</sub> at various sites shows that the net charge on adenine after interaction at the N- and NH<sub>2</sub>-sites is 0.139 and 0.041, respectively, showing that adenine acts as an electron donor in the interaction.

The HOMO-LUMO plots, shown in **Fig. 2(a)**, indicate that, in all the cases, the HOMO is localized on the QD. The LUMOs are also on (CdSe)<sub>3</sub>, implying that (CdSe)<sub>3</sub> QD is still electron deficient due to insufficient charge transfer from the nucleobase. The exceptions are the cases of interactions at the N and NCN sites, where the LUMO lies on the base. In both these cases, relatively larger negative charge transfer from adenine to (CdSe)<sub>3</sub> occurs and this is the reason for the adsorption being more exothermic in these two cases.

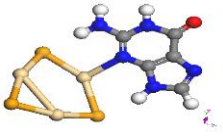
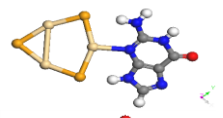
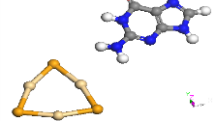
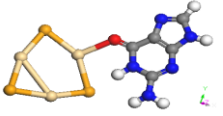
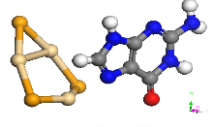
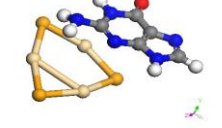
**Fig. 2(a)** HOMO (left) and LUMO (right) plots for interaction between (CdSe)<sub>3</sub> QD and adenine.



### (CdSe)<sub>3</sub>-Guanine interaction

Interaction of (CdSe)<sub>3</sub> with guanine at six possible sites is shown in **Table 2(b)**.

**Table 2(b).** Optimized structures of interaction between (CdSe)<sub>3</sub> QD and guanine and the energies (eV) involved.

Site	Final geometry	Interaction energy	HOMO	LUMO
N-site		0.54	-5.07	-2.38
NCN-site		0.46	-4.97	-2.27
NH <sub>2</sub> -site		-0.23	-5.05	-2.84
O-site		0.48	-4.54	-1.99
Five-membered ring		0.05	-4.36	-1.87
Six-membered ring		0.01	-4.93	-2.62

From **Table 2(b)**, it is observed that the interaction is exothermic [60] and N, NCN and O-sites are the preferred sites of interactions. Interaction at the N-site leads to bond formation between Cd6 of the QD and N3 of the base (bond order 0.272) of bond length 2.440 Å. A new Cd-Cd bond also forms, and its bond length is 3.210 Å. The average Cd-Se bond length is increased to 2.556 Å. Similar structural changes are observed when the NCN site interacts with the (CdSe)<sub>3</sub> QD. The Cd6-N3 bond length is 2.439 Å and its bond order is 0.272. The average Cd-Se bond length increase slightly (2.538 Å) and the Cd-Cd bond length of the newly formed bond is 3.210 Å. A Cd6-(6)O bond of bond order 0.254 develops on interaction via the O site. One Cd-Cd bond also forms. No bond formation between (CdSe)<sub>3</sub> and the base occurs in the rest of the cases; however, other structural changes in the QD are produced in all cases.

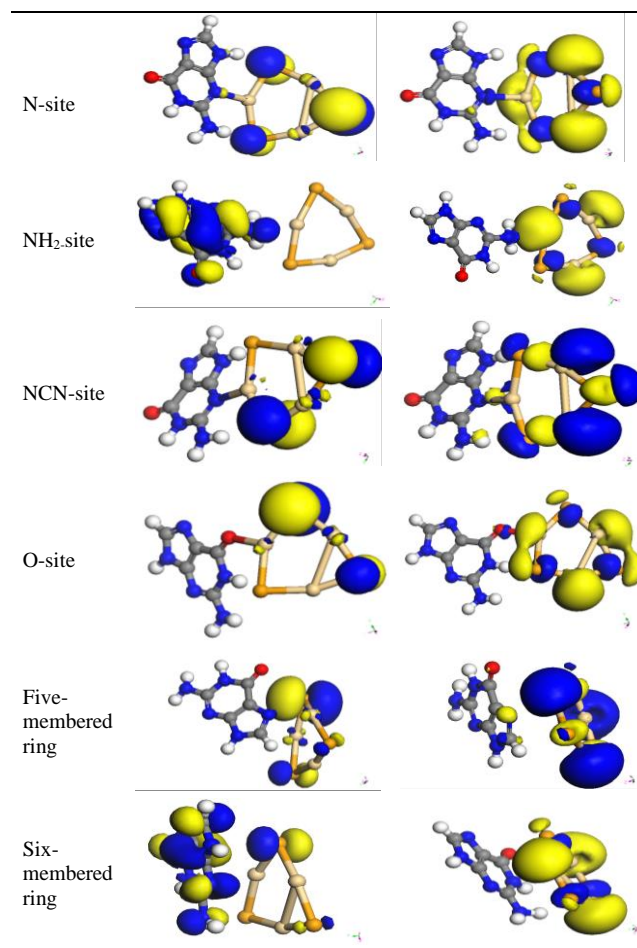
The calculated HOMO and LUMO energies of the structures after interaction are also shown in **Table 2(b)**. As shown in **Table 1**, guanine has the highest HOMO and LUMO energies amongst all the nucleobases, which makes it the best electron donor and poorest electron

acceptor. The low band gap implies that interaction at the NH<sub>2</sub>-site (2.21eV) is kinetically the least stable, while the interaction at the NCN and N-sites (2.69 and 2.70 eV) is both kinetically and thermodynamically favorable.

The Hirshfeld charge analysis indicates the maximum electron transfer from base to QD in case of five-membered ring interaction (0.166) due to the highest HOMO energy and least transfer when the interaction occurs at N-site (0.020), due to its very low HOMO energy, while the charge transfer shows an opposite trend (QD to guanine) in case of interaction with the six-membered ring of base. Although the charge transfer is smaller in this case than that in the case of adenine, electron transfer from the base to (CdSe)<sub>3</sub> occurs and hence it is an exothermic interaction.

The frontier orbital plots, shown in **Fig. 2(b)**, show that both the HOMO and LUMO are localized on (CdSe)<sub>3</sub> in all the cases, except in case of interaction at the NH<sub>2</sub>-site, where the HOMO lies on the base and it lies on both (i.e., base as well as QD) when the six-membered ring of the base interacts. The localization of the frontier orbitals majorly on (CdSe)<sub>3</sub> implies that any reaction after interaction of guanine with (CdSe)<sub>3</sub> would only affect (CdSe)<sub>3</sub> and does not damage the nucleobase.

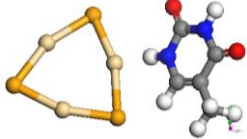
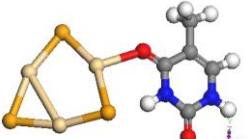
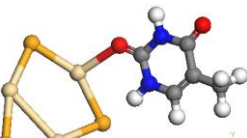
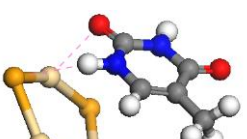
**Fig. 2(b).** HOMO (left) and LUMO (right) plots for interaction between (CdSe)<sub>3</sub> QD and guanine.



### (CdSe)<sub>3</sub>-Thymine interaction

In case of (CdSe)<sub>3</sub>-thymine interaction, the four possible sites of interaction are given in **Table 2(c)**. Thymine has two different kinds of oxygen atoms, which have been designated as (4)O (attached to C4 of base), and (2)O (attached to C2 of base).

**Table 2(c).** Optimized structures of interaction between (CdSe)<sub>3</sub> QD and thymine and the energies (eV) involved.

Site	Final geometry	Interaction Energy	HOMO	LUMO
N-site		-0.32	-5.07	-2.56
(4)O-site		0.15	-4.62	-2.26
(2)O-site		0.24	-4.75	-2.22
Top-site		0.00	-4.91	-2.47

The interaction between thymine and the (CdSe)<sub>3</sub> QD is exothermic for all cases (**Table 2(c)**), except when it occurs at the N-site (N1 of base). The interaction energies are smaller than the previous two cases of adenine and guanine. The highest value is for interaction at the (2)O-site.

No bond formation and no increase in covalency are observed when the N-site (N1 of base) of the base interacts with the (CdSe)<sub>3</sub> QD. The average Cd-Se bond length decreases to 2.528 Å. An increase in covalency of the cadmium atoms is observed in the rest of the cases due to formation of a Cd-Cd bond. Bond formation between an atom of the base and the QD is observed only in case of (4)O-site (bond order 0.200) and (2)O-site (bond order 0.204), with Cd-O bond lengths equal to 3.208 Å and 3.240 Å, respectively, while a weaker interaction is observed between Cd and (2)O, with a separation of 2.717 Å and a bond order of 0.143 when thymine is placed on top of (CdSe)<sub>3</sub>. The average Cd-Se bond length is increased to 2.540 Å, 2.547 Å, and 2.540 Å respectively in

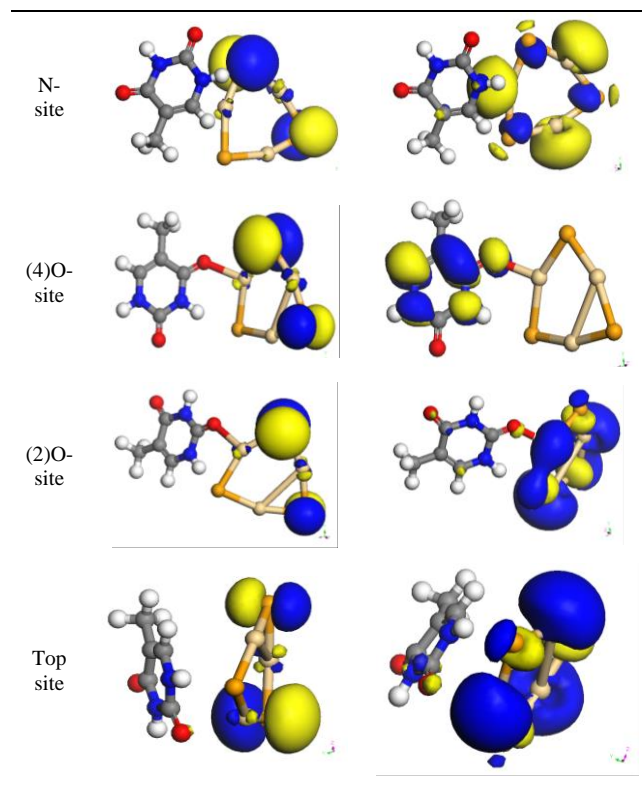
case of top-site, (4)O-site, and (2)O-site interactions, while very minor changes in the bond lengths of thymine are observed.

Thymine has a lower HOMO energy than (CdSe)<sub>3</sub> (**Table 1**) indicating that it is unable to donate much charge to (CdSe)<sub>3</sub>. However, its LUMO energy is higher than that of (CdSe)<sub>3</sub> QD. Because of the poorer electron donation by thymine, its HOMO energy remains low. The Hirshfeld charge analysis confirms the same and shows negligible charge transfer from thymine. The maximum charge transfer from the base to (CdSe)<sub>3</sub> QD occurs on interaction at the (4)O site, with the net charge on thymine at the (4)O-site being 0.064, followed by N-site and (2)O-site, in both of which cases, the charge transfer is 0.054.

The HOMO and LUMO contours are shown in **Fig. 2(c)**. The HOMOs and LUMOs lie on (CdSe)<sub>3</sub> in all the cases, except in case of the (4)O-site, where the LUMO lies on thymine, although there is some delocalization of the LUMO on thymine in other cases as well.

Interaction at the N and (2)O-site is kinetically favored due to higher HOMO-LUMO gaps (2.51 and 2.53 eV, respectively) compared to the bare QD (2.49 eV), whereas the (2)O-site interaction is thermodynamically favorable as well.

**Fig. 2(c).** HOMO (left) and LUMO (right) plots for interaction between (CdSe)<sub>3</sub> QD and thymine.

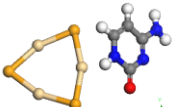
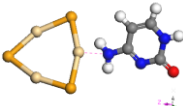
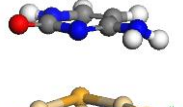
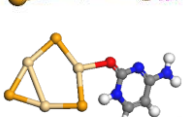


### (CdSe)<sub>3</sub>-Cytosine interaction

Four possible sites were explored for the interaction of cytosine with (CdSe)<sub>3</sub> QD (**Table 2(d)**).



**Table 2(d).** Optimized structures of interaction between the (CdSe)<sub>3</sub> QD and cytosine and the energies (eV) involved.

Site	Final geometry	Interaction Energy	HOMO	LUMO
N-site		-0.17	-4.81	-2.30
NH <sub>2</sub> -site		0.02	-4.89	-2.37
Top-site		-0.04	-4.84	-2.47
O-site		0.51	-4.48	-1.97

No bond formation between the two occurs when the N-site (N1) of the base interacts and when cytosine is placed on the top of the QD ring, while only a close contact between Cd6 of the QD and (4)N of base of distance 2.764 Å and bond order 0.137 occurs when interaction occurs at the NH<sub>2</sub>-site. A bond between Cd6 and (2)O of bond length 2.357 Å and bond order 0.256 is formed only in case of O-site interaction. Structural reorganization also occurs in the nucleobase, and relatively smaller changes in the QD, as seen from the interaction energies. The data given in **Table 2(d)** shows that the cytosine-(CdSe)<sub>3</sub> interaction is exothermic for interaction at the NH<sub>2</sub>- and O-sites, and is endothermic for interaction at N-site and when the base interacts from the top. The maximum interaction is observed in case of O-site.

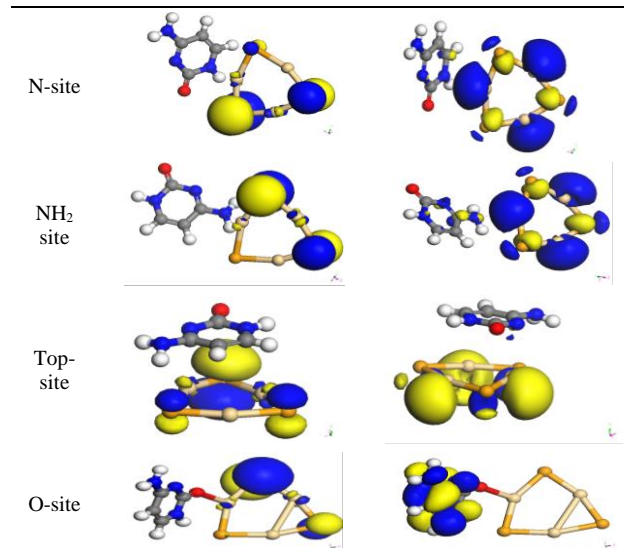
The calculated electronic properties are also given in **Table 2(d)**. Interaction at the N, NH<sub>2</sub> and O-sites are kinetically favored because of the enhancement in the HOMO-LUMO gaps (2.51, 2.52 and 2.51 eV, respectively) while interaction at the O-site is thermodynamically favorable as well.

The frontier orbital plots, given in **Fig. 2(d)**, show that both the HOMO and LUMO are localized on (CdSe)<sub>3</sub>, except in case of O-site interaction, where the LUMO lies on cytosine. However, there is some delocalization of the LUMO on cytosine in other cases also.

Because of the higher HOMO energy of cytosine than thymine, it is a better electron donor than thymine, and hence higher charge transfer to (CdSe)<sub>3</sub> can take place, making it less electron deficient. The Hirshfeld charge analysis for interaction of cytosine with (CdSe)<sub>3</sub> at various sites shows that the net charge on cytosine for interaction at the N, NH<sub>2</sub> and O-sites is 0.088, 0.091 and 0.093, respectively, showing that cytosine also acts as an electron donor in the interaction.

The localization of the frontier orbitals on (CdSe)<sub>3</sub> implies that any reaction of the resultant structure after interaction would only affect (CdSe)<sub>3</sub> and does not damage the nucleobase.

**Fig. 2(d).** HOMO (left) and LUMO (right) plots for interaction between cytosine and (CdSe)<sub>3</sub> QD.



### (CdSe)<sub>3</sub>-Uracil interaction

Four sites were considered for studying the interaction of uracil with the QD (**Table 2(e)**). Like thymine, uracil also has two kinds of oxygen atoms and we have designated them as (4)O (attached to C4 of uracil), and (2)O (attached to C2 of uracil).

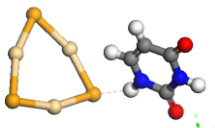
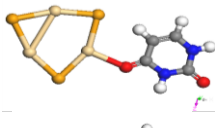
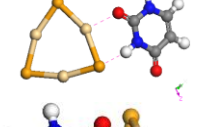
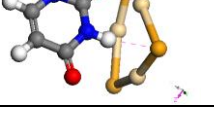
As shown in **Table 2(e)**, the interaction is strongest for the (4)O-site, where a weak bond is formed between Cd4 and (4)O of bond length 2.471 Å and bond order 0.177, and an increase in covalency of all cadmium atoms also occurs. For interaction via the (2)O-site, contacts are formed between Se5-(3)H and Cd4-(2)O with bond distances 2.508 Å (bond order 0.167) and 2.476 Å (bond order 0.174), respectively. For the N-site, a contact between Se3-(1)H with bond distance 2.642 Å (bond order 0.133) is observed. In case of the top-site interaction, contacts between Se1-(3)H and Cd2-(2)O with bond distances 2.535 Å (bond order 0.168) and 2.533 Å (bond order 0.163), respectively, are observed.

Although the interaction energies for various sites do not differ much, it can be inferred that interactions at the (4)O and (2)O sites lead to more stable structures. The data for the interaction energies (**Table 2(e)**) shows that the interaction is exothermic for all orientations, except at the N-site. Interaction at the top site is the most favorable interaction kinetically (band gap 2.48 eV) while thermodynamically the most favorable interaction is at the (4)O-site.

Uracil has the lowest LUMO energy among all the nucleobases (**Table 1**), and hence is the only nucleobase capable of accepting electron density from the QD. This is confirmed by Hirshfeld charge analysis also. Although the

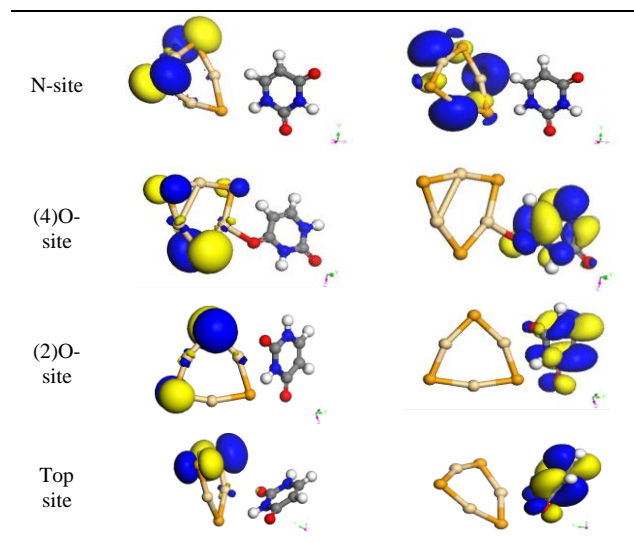
charge transfer is small, this is the only nucleobase which accepts electron density from the QD, particularly for the N-site interaction, where the charge on the base is -0.148 after interaction with the QD, leaving the QD electron deficient, resulting in both the HOMO and LUMO lying on the QD (**Fig. 2(e)**). However, for the most favorable (4)O interaction, the QD again acts as an electron acceptor, accepting electron density from the lone pairs of the C4 oxygen of uracil with the charge on the base being 0.015.

**Table 2(e)** Optimized structures for interaction between (CdSe)<sub>3</sub> QD and uracil and the energies (eV) involved.

Site	Final geometry	Interaction energy	HOMO	LUMO
N-site		-0.04	-5.35	-2.94
(4)O-site		0.16	-4.58	-2.51
(2)O-site		0.15	-4.68	-2.22
Top-site		0.11	-4.69	-2.21

The HOMO and LUMO contours are shown in **Fig. 2(e)**. These show that, while the HOMO lies on (CdSe)<sub>3</sub>, the LUMO lies mainly on uracil, except in case of the unfavorable N-site interaction, indicating that the base remains the site of nucleophilic attack.

**Fig. 2(f)**, HOMO (left) and LUMO (right) plots for interaction between (CdSe)<sub>3</sub> QD and uracil.



## Vibrational analysis

The vibrational spectra calculated for the (CdSe)<sub>3</sub>-nucleobase systems are shown in **Fig. 3(a-e)**. Here, we have given the vibrational spectrum of only the most exothermic interaction of each nucleobase and compared it to the spectrum of the bare (CdSe)<sub>3</sub> QD. The spectra have been magnified and overlapped with those obtained for the (CdSe)<sub>3</sub> QD to show the shift in the vibrational peaks.

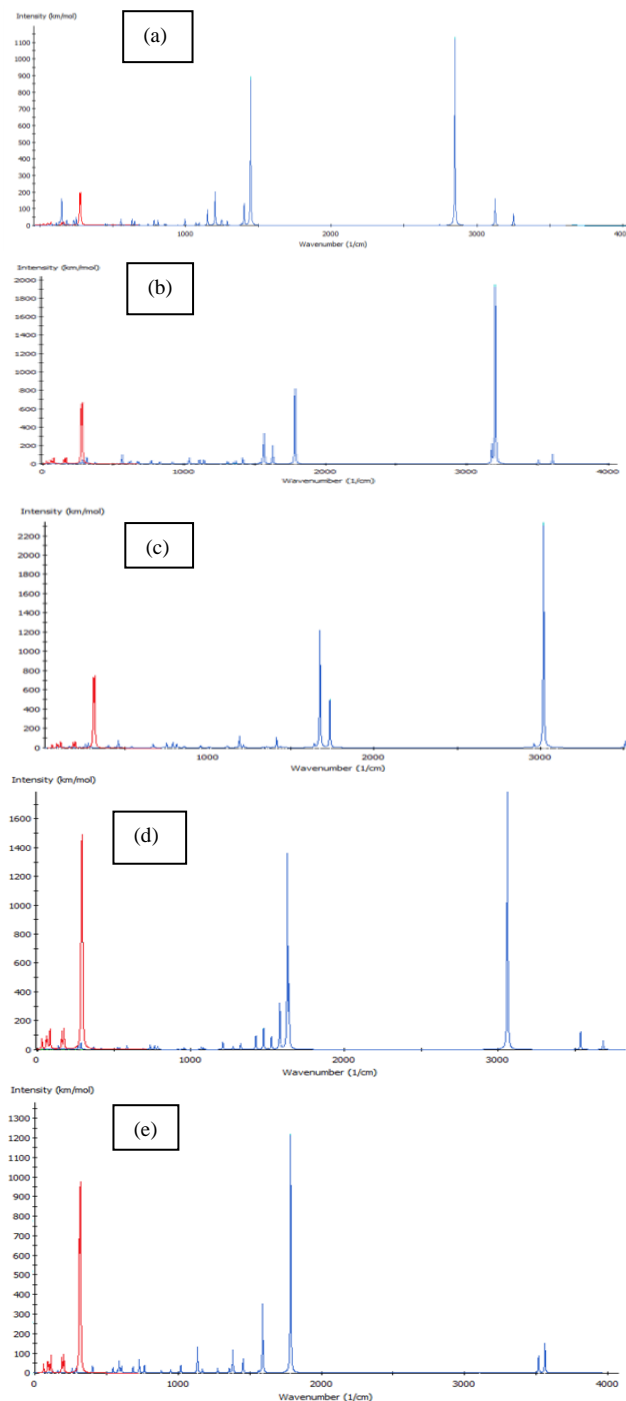


**Fig. 3.** Vibrational spectra in red (for bare (CdSe)<sub>3</sub> QD) and blue (for (CdSe)<sub>3</sub> QD with nucleobase) for (a) (CdSe)<sub>3</sub>-adenine (b) (CdSe)<sub>3</sub>-guanine (c) (CdSe)<sub>3</sub>-thymine (d) (CdSe)<sub>3</sub>-cytosine (e) (CdSe)<sub>3</sub>-uracil.



Though various peaks were observed as a result of ring distortions but in each interaction, the most intense peak observed can be attributed to a particular stretch. In case of (CdSe)<sub>3</sub>-Adenine interaction, the peaks were found at 989cm<sup>-1</sup>, 1075cm<sup>-1</sup>, 1144cm<sup>-1</sup>, and 1,301 cm<sup>-1</sup> and the strong intensity peaks at 1,385, 1,556, and 1,617 cm<sup>-1</sup> can be attributed to  $\nu(\text{C-N})$  and  $\nu(\text{C-C})$  vibrations [67] whereas the most intense peak at 3222 cm<sup>-1</sup> is due to the symmetric stretch of NH<sub>2</sub> group. For (CdSe)<sub>3</sub>-Guanine interaction, strong peaks at 1,671 and 1,694 cm<sup>-1</sup> can be allocated to  $\nu(\text{C=O})$  vibrations and the intense peak at 3203 cm<sup>-1</sup> is due to the symmetric stretch of NH<sub>2</sub> group. For (CdSe)<sub>3</sub>-Thymine interaction, peaks below 100 cm<sup>-1</sup> can be owed to the ring deformations while peaks at 1748 cm<sup>-1</sup> and 1819 cm<sup>-1</sup> are assigned to C=O vibrations. The most intense peak at 3019 cm<sup>-1</sup> in this also is due to the  $\nu(\text{NH}_2)$  vibrations. Like in all the interactions, low frequency peaks, are due to ring deformations, so is the case of cytosine. Here, robust peaks which are observed at 1390 cm<sup>-1</sup>, 1,480 cm<sup>-1</sup>, and 1608 cm<sup>-1</sup> can be considered to be due to  $\nu(\text{C-N})$  and  $\nu(\text{C=O})$  vibrations. A peak at around 1180 cm<sup>-1</sup> can be assigned to the rocking N-H vibration whereas the most intense peak at 3060 cm<sup>-1</sup> is due to the symmetric stretch of N-H bond. For (CdSe)<sub>3</sub>-Uracil interaction, as can be seen from the spectra, along with the lower frequency vibrations, the most intense peak is observed at 1656 cm<sup>-1</sup>, which is due to the symmetric stretch of the (4)O-C4 bond and in-plane bending vibration of hydrogens.

The vibrational data for the most intense peak in each case is given in **Table 3**. The most intense peak is due to the symmetric stretch of the N-H bond of the nucleobase, but for uracil, the most intense peak is due to the symmetric stretch of the (4)O-C4 bond and in-plane bending vibration of hydrogens. Interaction with the QD weakens the C4 carbonyl bond, reducing its wavenumber from the normal carbonyl frequency. The vibrational frequency data show that in all the cases, the intensities of the peaks for the (CdSe)<sub>3</sub> QDs increase on interaction with various nucleobases, with the largest increase in case of the (CdSe)<sub>3</sub>-thymine interaction. This can be explained from the energies of the HOMOs and LUMOs, while thymine has a higher lying LUMO, the charge transfer is in the reverse direction, i.e., from the QD to the nucleobase in case of uracil and hence the lower intensity of the peak in uracil may be attributed to the lower lying LUMO of uracil.

By looking at the vibrational spectra, we observe a blue shift after interaction in all the cases. The shifting of the peak was caused by the increased size of the QDs after the interaction with the bases. The sizes of (CdSe)<sub>3</sub>-Purine were found to be much bigger than that of (CdSe)<sub>3</sub>-Pyrimidine, that has been reflected in the shifting of the peaks. When (CdSe)<sub>3</sub>-nucleobase combined system is compared with the individual (Cdse)<sub>3</sub> system, the HOMO-LUMO gap of the combined system is larger (considering the most stable site obtained in this work), i.e., it is observed that on comparing with the infrared data of the

free (CdSe)<sub>3</sub> quantum dot with the combined system of (CdSe)<sub>3</sub>-nucleobase, there were shifts observed to higher frequencies, perhaps due to the coordination of the molecules to the surface of the quantum dot or due to nearly some interactions that occur among them.

**Table 3.** Vibrational data for peaks corresponding to maximum intensity.

(CdSe) <sub>3</sub> -Base	Frequency (cm <sup>-1</sup> )	Intensity (km mol <sup>-1</sup> )
Bare (CdSe) <sub>3</sub>	280	34
(CdSe) <sub>3</sub> -Adenine	3222	1135
(CdSe) <sub>3</sub> -Guanine	3203	1953
(CdSe) <sub>3</sub> -Thymine	3019	2364
(CdSe) <sub>3</sub> -Cytosine	3060	1885
(CdSe) <sub>3</sub> -Uracil	1656	883

## Conclusions

The present work has focused on the application of the (CdSe)<sub>3</sub> QD, the smallest wurtzite nanocluster, as a DNA sensor. This has been employed as a benchmark to test the model systems. We have studied the interaction of the (CdSe)<sub>3</sub> QD with various purines and pyrimidine bases present in nucleic acids. Our calculated results provide a bridge between the atomistic details of bioconjugation and the corresponding optical properties.

We have considered various possible sites of interaction for each nucleobase. Our calculations predict that out of all the nucleobases considered, the binding of (CdSe)<sub>3</sub> to guanine is strongest, and with uracil is weakest, because of the smallest energy gap between the HOMO of guanine and the LUMO of the QD (i.e., 2.09 eV), and the largest gap in the case of uracil (i.e., 2.99 eV), which prevents adequate charge transfer to the QD. While in the other cases, weak bonds are formed between cadmium and an oxygen or nitrogen atom of the nucleobase with very little transfer of electron density from the nucleobase to the QD, the opposite occurs in the case of uracil. As predicted from the energies of the HOMOs and LUMOs, in this case the charge transfer is in the opposite direction, i.e., from the QD to the nucleobase. In the case of uracil, the low-lying LUMO of the nucleobase is conducive to electron transfer from the QD to the base. The other two pyrimidines, cytosine and thymine, have higher lying LUMOs, making such electron transfer difficult.

The vibrational analysis of the combined systems, when compared with that of the bare (CdSe)<sub>3</sub> QD, shows that the intensities of the peaks due to (CdSe)<sub>3</sub> increase on interaction with nucleobases, and a blue-shift is observed in all interactions. The observed shift is in good agreement with the experimental findings. This suggests that our results are reasonably matching the real QDs.

We have seen that the Cd<sub>3</sub>Se<sub>3</sub> QDs binds strongly with the DNA/RNA nucleobase molecules owing to the presence of various chemical moieties such as carbonyl, heterocyclic and amide groups, thereby display strong

binding interaction with CdSe QDs. This also implies, that these nucleobases can be layered stably over the CdSe QDs. Hence, a moderately strong intensity of emission spectra can be expected at a relatively low concentration of nucleobase molecules. Since the (CdSe)<sub>3</sub> QDs interacts differently with each of the nucleobases, hence the spectra of the QDs after the interaction with entire DNAs/RNAs should be observed at different frequencies in the case of diverse sequences. This proves that CdSe quantum dots can suitably be used as promising materials to detect any change in the DNA sequence, any mutations or any damage to the DNA molecules. Regarding the question of DNA damage, we actually see that (CdSe)<sub>3</sub> acts as a protector of DNA from damage, since in most of the complexes, both the frontier orbitals lie on the QD, implying that this is the site of external attack and the DNA base is relatively safe.

#### Acknowledgements

PM thanks the Council for Scientific and Industrial Research (CSIR), New Delhi, India, for a Senior Research Fellowship under Grant No. 09/045(0873)/2009 EMR-I. Also, monetary support from "Delhi University's system to build up Research by providing resources to Faculty" is appreciatively acknowledged.

#### Conflicts of interest

There are no conflicts to declare.

#### Keywords

Nucleobase, purine, pyrimidine, quantum dots, sensing, HOMO, LUMO

#### Abbreviations

QDs, Quantum Dots; A, Adenine; G, Guanine; C, Cytosine; T, Thymine; U, Uracil; DFT, Density Functional Theory; DNA, Deoxyribonucleic acid; RNA, Ribonucleic acid; HOMO, Highest occupied molecular orbital; LUMO, Lowest unoccupied molecular orbital.

Received: 23 February 2021

Revised: 18 April 2021

Accepted: 26 April 2021

#### References

- Wang, H.S.; Ju, H.X.; Chen, H.Y.; *Anal. Chim. Acta*, **2002**, *461*, 243.
- Kuroda, N.; Nakashima, K.; Akiyama, S.; *Anal. Chim. Acta*, **1993**, *278*, 275.
- Tseng, H. C.; Dadoo, R.; Zare, R. N.; *Anal. Biochem.*, **1994**, *222*, 55.
- Jin, W.; Wei, H.; Zhao, X.; *Electroanalysis*, **1997**, *9*, 770.
- Xu, D.K.; Hua, L.; Chen, H.Y.; *Anal. Chim. Acta*, **1996**, *335*, 95.
- Huang, X.; El-Sayed, I. H.; Qian, W.; El-Sayed, M. A.; *Nano Lett.*, **2007**, *7*, 1591.
- Nagasaki, Y.; *Chem. Lett.*, **2008**, *37*, 564.
- Oberdörster, G.; Oberdörster, E.; Oberdörster, J.; *Environ. Health Perspect.*, **2005**, *113*, 823.
- Le, J. D.; Pinto, Y.; Seeman, N. C.; Musier-Forsyth, K.; Talon, T. A.; Kiehl, R. A.; *Nano Lett.*, **2004**, *4*, 2343.
- Pinto, Y. Y.; Le, J. D.; Seeman, N. C.; Musier-Forsyth, K.; Taton, T. A.; Kiehl, R. A.; *Nano Lett.*, **2005**, *5*, 2399.
- Sharma, J.; Chhabra, R.; Liu, Y.; Ke, Y.; Yan, H.; *Angew. Chem. Int. Ed.*, **2006**, *45*, 730.
- Whaley, S. R.; English, D. S.; Hu, E. L.; Barbara, P. F.; Belcher, A. M.; *Nature*, **2000**, *405*, 665.
- Artemyev, M.; Kisiel, D.; Abmriotko, S.; Antipina, M. N.; Khomutov, G. B.; Kislov, V. V.; Rakhnyanskaya, A. A.; *J. Am. Chem. Soc.*, **2004**, *126*, 10594.
- Bakalova, R.; Ohba, H.; Zhelev, Z.; Nagase, T.; Jose, R.; Ishikawa, M.; Baba, Y.; *Nano Lett.*, **2004**, *4*, 1567.
- Chen, F.; Gerion, D.; *Nano Lett.*, **2004**, *4*, 1827.
- Chung, S. Y.; Lee, S.; Liu, C.; Neuhauser, D.; *J. Phys. Chem. B*, **2009**, *113*, 292.
- Clapp, A. R.; Medintz, I. L.; Fisher, B. R.; Anderson, G. P.; Mattoussi, H.; *J. Am. Chem. Soc.*, **2005**, *127*, 1242.
- Freeman, R.; Finder, T.; Bahshi, L.; Willner, I.; *Nano Lett.*, **2009**, *9*, 2073.
- Gill, R.; Willner, I.; Shweky, I.; Banin, U.; *J. Phys. Chem. B*, **2005**, *109*, 23715.
- Gill, R.; Zayats, M.; Willner, I.; *Angew. Chem., Int. Ed.*, **2008**, *47*, 7602.
- Klimov, V.I.; Mikhailovsky, A.A.; Xu, S.; Malko, A.; Hollingsworth, J. A.; Leatherdale, C. A.; Eisler, H. J.; Bawendi, M. G.; *Science*, **2000**, *290*, 314.
- Liu, P.; Wang, Q.; Li, X.; *J. Phys. Chem. C*, **2009**, *113*, 7670.
- Ma, N.; Yang, J.; Stewart, K. M.; Kelley, S. O.; *Langmuir*, **2007**, *23*, 12783.
- Mattoussi, H.; Mauro, J. M.; Goldman, E. R.; Anderson, G. P.; Sundar, V. C.; Mikulec, F. V.; Bawendi, M. G.; *J. Am. Chem. Soc.*, **2000**, *122*, 12142.
- Michalet, X.; Pinaud, F. F.; Bentolila, L. A.; Tsay, J. M.; Doose, S.; Li, J. J.; Sundaresan, G.; Wu, A. M.; Gambhir, S. S.; Weiss, S.; *Science*, **2005**, *307*, 538.
- Patolsky, F.; Gill, R.; Weizmann, Y.; Mokari, T.; Banin, U.; Willner, I.; *J. Am. Chem. Soc.*, **2003**, *125*, 13918.
- Pinaud, F.; King, D.; Moore, H. P.; Weiss, S.; *J. Am. Chem. Soc.*, **2004**, *126*, 6115.
- Sandros, M. G.; Gao, D.; Benson, D. E.; *J. Am. Chem. Soc.*, **2005**, *127*, 12198.
- Smith, A. M.; Ruan, G.; Rhyner, M. N.; Nie, S.; *Ann. Biomed. Eng.*, **2006**, *34*, 3.
- Tsay, J. M.; Doose, S.; Weiss, S.; *J. Am. Chem. Soc.*, **2006**, *128*, 1639.
- Malik, P.; Kakkar, R.; *J. Nanopart. Res.*, **2018**, *20*, 4.
- Malik, P.; Gulia, S.; Kakkar, R.; *Adv. Mater. Lett.*, **2013**, *4*, 811.
- Parak, W. J.; Gerion, D.; Pellegrino, T.; Zanchet, D.; Mischeel, C.; Williams, S.C.; Boudreau, R.; Le Gros, M.A.; Larabell, C.A.; Alivisatos, A. P.; *Nanotechnology*, **2003**, *14*, R15.
- Murray, C. B.; Norris, D. J.; Bawendi, M. G.; *J. Am. Chem. Soc.*, **1993**, *115*, 8706.
- Wang, Z.; Xiao, S.; Chen, Y.; *J. Electroanal. Chem.*, **2006**, *589*, 237.
- Wu, K.; Fei, J.; Bai, W.; Hu, S.; *Anal. Bioanal. Chem.*, **2003**, *376*, 205.
- Kim, H.S.; Jang, S.W.; Chung, S.Y.; Lee, S.; Lee, Y.; Kim, B.; Liu, C.; Neuhauser, D.; *J. Phys. Chem. B*, **2010**, *114*, 471.
- Zhu, H.; Zhao, G.C.; *Microchim. Acta*, **2009**, *165*, 329.
- Kalaivani, A.; Narayanan, S.S.; *J. Nanosci. Nanotechnol.*, **2015**, *15*, 4697.
- Xuejiao, F.; Qingkun, S.; Hongjian, L.; Hongdan, W.; Wenlan, W.; Zhidan, W.; *J. Phys. Chem. C*, **2009**, *113*, 6929.
- Xuejiao, F.; Qingkun, S.; Hongjian, L.; Wenlan, W.; Zhidan, W.; Junyu, L.; *J. Lumin.*, **2010**, *130*, 648.
- Chanu, T. I.; Negi, D.P.S.; *Chem. Phys. Lett.*, **2010**, *491*, 75.
- Sieberg, D.; Herten, D. P.; *Aust. J. Chem.*, **2011**, *64*, 512.
- Baylin, S. B.; Ohm, J. E.; *Nat. Rev. Cancer*, **2006**, *6*, 107.
- Duffy, M. J.; Napieralski, R.; Martens, J. W.; Span, P. N.; Spyrtos, F.; Sweep, F. C.; Brunner, N.; Foekens, J. A.; Schmitt, M.; *Eur. J. Cancer*, **2009**, *45*, 335.
- Mulero-Navarro, S.; Esteller, M.; *Crit. Rev. Oncol. Hematol.*, **2008**, *68*, 1.
- Zhang, J.; Xing, B.; Song, J.; Zhang, F.; Nie, C.; Jiao, L.; Liu, L.; Lv, F.; Wang, S.; *Anal. Chem.*, **2014**, *86*, 346.
- Hosseini, M.; Khaki, F.; Shokri, E.; Khabbaz, H.; Dadmehr, M.; Ganjali, M. R.; Feizabadi, M.; Asjlou, D.; *J. Fluoresc.*, **2017**, *27*, 2059.
- Moullick, A.; Milosavljevic, V.; Vlachova, J.; Podgajny, R.; Hynek, D.; Kopel, P.; Adam, V.; *Int. J. Nanomedicine*, **2017**, *12*, 1277.
- Li, G.; Fei, X.; Liu, H.; Gao, J.; Nie, J.; Wang, Y.; Tian, Z.; He, C.; Wang, J. L.; Ji, C.; Oron, D.; Yang, G.; *ACS Nano*, **2020**, *14*, 4196.

51. Faramarzi, V.; Ahmadi, V.; Fotouhi, B.; Abasifard, M.; *Scientific Reports*, **2019**, 9, 6230.
52. Rodzik-Czalka, L.; Lewandowska-Łańcucka, J.; Gatta, V.; Nowakowska, M.; *J. Colloid Interface Sci.*, **2018**, 514, 479.
53. Kumar, M.; Thakur, N.; Sharma, M.; AIP Conference Proceedings, **2020**, 2265, 030352.
54. Sharma, B.; Mandani, S.; Thakur, N.; Sarma, T. K.; *Soft Matter*, **2018**, 14, 5715.
55. Saha, S.; Sarkar, P.; *Phys. Chem. Chem. Phys.*, **2014**, 16, 15355.
56. Hohenberg, P.; Kohn, W.; *Phys. Rev. B*, **1964**, 136, B864.
57. Delley, B.; *J. Chem. Phys.*, **1990**, 92, 508.
58. Delley, B.; *J. Chem. Phys.*, **1991**, 94, 7245.
59. Delley, B.; *J. Comp. Chem.*, **1996**, 17, 1152.
60. Delley, B.; *J. Chem. Phys.*, **2000**, 113, 7756.
61. Delley, B.; *Phys. Rev. B*, **2002**, 66, 155125/1.
62. Matsuzawa, N.; Seto, J.; Dixon, D. A.; *J. Phys. Chem. A*, **1997**, 101, 9391.
63. Batra, P.; Gaba, R.; Issar, U.; Kakkar, R.; *Journal of Theoretical Chemistry*, **2013**, 2013, 14 pages.
64. Hirshfeld, F. L.; *Isr. J. Chem.*, **1977**, 16, 198.
65. Mayer, I.; *Int. J. Quantum Chem.*, **1986**, 29, 477.
66. Kakkar, R.; Kapoor, P. N.; Klabunde, K. J.; *J. Phys. Chem. B*, **2004**, 108, 18140.
67. Nowak, M. J.; Lapinski, L.; Kwiatkowski, J. S.; Leszczynski, J.; *J. Phys. Chem.*, **1996**, 100, 3527.

#### Authors biography



**Dr. Pragati Malik**, an Assistant Professor in Acharya Narendra Dev College, University of Delhi, has done her B.Sc. (2007) and M.Sc. (2009) in Physical Chemistry (specialization) from Delhi University, India and has completed her Ph.D. under supervision of Prof. Rita Kakkar from University of Delhi in 2014. Her research interests include theoretical studies of nanomaterials, particularly CdSe quantum dots and their interaction with various chemical and bioanalyses in order to develop novel chemical and biosensors.



**Rita Kakkar**, after obtaining a PhD degree in Physical Chemistry from the University of Delhi, undertook research on various topics. She has been teaching Physical Chemistry at the University of Delhi for the past three decades. Her main research interests are in Computational Chemistry and related fields. Professor Rita Kakkar has over 100 research publications in international journals. She also regularly reviews manuscripts for many international journals, including those published by the American Chemical Society, Royal Society of Chemistry, Wiley and Elsevier.

#### Graphical abstract

